

## Surface Structure of Liquid Li and Na: An *ab initio* Molecular Dynamics Study

D. J. González,<sup>1,2</sup> L. E. González,<sup>2</sup> and M. J. Stott<sup>1</sup>

<sup>1</sup>*Department of Physics, Queen's University, Kingston, Ontario, Canada K7L 3N6*

<sup>2</sup>*Departamento de Física Teórica, Facultad de Ciencias, Universidad de Valladolid, 47011 VA, Spain*

(Received 30 September 2003; published 23 February 2004)

Molecular dynamics simulations of the liquid-vapor interfaces of liquid metals have been performed using first principles methods. Results are presented for liquid lithium and sodium near their respective triple points, for samples of 2000 particles in a slab geometry. The atomic density profiles show a pronounced stratification extending several atomic diameters into the bulk, which is similar to that already experimentally observed in liquid K, Ga, In, and Hg.

DOI: 10.1103/PhysRevLett.92.085501

PACS numbers: 61.25.Mv, 64.70.Fx, 71.15.Pd

The study of the structure of the free liquid surface has attracted much theoretical and experimental work [1,2], with emphasis on the possible existence of liquid surface layers. Although it is now well established that ionic [3] and dielectric [1,4] liquids exhibit just a smooth monotonic decay from the bulk liquid density to the bulk vapor density, liquid surface layering appears in liquid crystals [5] and at the interface between a simple fluid and a hard wall [6]. Special attention has been devoted to liquid metals since the early experiments suggested a liquid surface layered structure in Hg [7]; computer simulation [8,9] and theoretical studies [10] predicted a significant structure, extending several atomic layers into the bulk liquid. These results have been recently corroborated by x-ray reflectivity experiments on liquid Hg, Ga, In, K, and Na<sub>0.33</sub>K<sub>0.67</sub> [11].

It is not clear whether surface layering is a feature of all liquid metals or only characteristic of some. Rice and co-workers [8] have performed Monte Carlo (MC) simulations based on pair potentials that depend on an electron density obtained self-consistently within density functional theory (DFT) [12]; their results suggest that surface layering is due to the coupling between ionic and electronic profiles and that the abrupt decay of the electron density profile gives rise to an effective wall against which the ions, behaving similar to hard spheres, stack. Other workers [13] have suggested that the many body forces arising from the delocalized electrons tend to increase the ionic surface density so that its coordination approaches that of the bulk. Recently, Chacon *et al.* [14] proposed that surface layering may be a generic property of fluids at low temperature, so that the only requirement for an oscillatory density profile is a low melting temperature relative to the critical temperature so as to avoid crystallization.

In this Letter, we present results for the liquid-vapor interface of pure liquid Li and Na at thermodynamic conditions near their respective triple points. This has been carried out by using the orbital-free *ab initio* molecular dynamics (OF-AIMD) method, where the forces acting on the nuclei are computed from electronic struc-

ture calculations, based on DFT, which are performed as the MD trajectory is generated. Large samples and long MD simulation times are possible when interatomic pair potentials are used to describe the effective ion-ion interactions, but at a liquid metal surface this approximation must break down as the electron density drops from its value in the bulk to zero outside the surface. In these circumstances, it is vital to allow the forces on the atoms to respond to the electron density distribution in their vicinity. The best way of accomplishing this is presently through the Kohn-Sham (KS) approach to density functional theory (KS-AIMD methods), but this approach is very time consuming, limiting the sample sizes and the simulation times; until now, only one KS-AIMD calculation has been performed which studied the liquid silicon surface by using 96 particles and lasted for 30 ps [9]. The OF-AIMD method uses an explicit approximation for the electron kinetic energy functional of DFT but otherwise correctly treats the forces on the ions. The approximation greatly simplifies the calculations allowing simulation of much larger samples for long times.

A simple liquid metal is treated as a disordered array of  $N$  bare ions with valence  $Z$ , enclosed in a volume  $V$ , and interacting with  $N_e = NZ$  valence electrons through electron-ion potentials. The total potential energy of the system can be written, within the Born-Oppenheimer approximation, as the sum of the direct ion-ion Coulombic interaction energy and the ground state energy of the electronic system,  $E_g[\rho_g(\vec{r})]$ . According to DFT, the ground state electronic density,  $\rho_g(\vec{r})$ , minimizes an energy functional which is given as the sum of the kinetic energy of independent electrons,  $T_s[\rho]$ , the classical Hartree electrostatic energy,  $E_H[\rho]$ , the exchange-correlation energy,  $E_{xc}[\rho]$ , for which we have adopted the local density approximation, and, finally, the electron-ion interaction energy,  $E_{\text{ext}}[\rho]$ , for which we have used ionic pseudopotentials which are local (as required by the lack of orbitals) but constructed within DFT [15].

In the KS-DFT method [12],  $T_s[\rho]$  is calculated exactly by using single particle orbitals, which require huge computational effort. This is alleviated in the OF-AIMD

approach [12,15,16] by use of an explicit but approximate functional of the electronic density for  $T_s[\rho]$ . Proposed functionals consist of the von Weizsäcker term,  $T_W[\rho(\vec{r})] = \frac{1}{8} \int d\vec{r} |\nabla \rho(\vec{r})|^2 / \rho(\vec{r})$ , plus further terms chosen in order to reproduce correctly some exactly known limits. Here, we have used an average density model [15], where  $T_s = T_W + T_\beta$ :

$$T_\beta = \frac{3}{10} \int d\vec{r} \rho(\vec{r})^{5/3-2\beta} \tilde{k}(\vec{r})^2, \quad (1)$$

$$\tilde{k}(\vec{r}) = (2k_F^0)^3 \int d\vec{s} k(\vec{s}) w_\beta(2k_F^0|\vec{r} - \vec{s}|).$$

$k(\vec{r}) = (3\pi^2)^{1/3} \rho(\vec{r})^\beta$ ,  $k_F^0$  is the Fermi wave vector for mean electron density  $\rho_e = N_e/V$ , and  $w_\beta(x)$  is a weight function chosen so that both the linear response theory and Thomas-Fermi limits are correctly recovered. Another key ingredient is the local ion pseudopotential,  $v_{ps}(r)$ , describing the ion-electron interaction; it has been developed from first principles by fitting, within the same  $T_s[\rho]$  functional, the displaced electronic density induced by an ion immersed in a metallic medium as obtained in a KS calculation [15]. The combination of this local pseudopotential along with the previous  $T_s[\rho]$  functional has provided an accurate description of several static and dynamic properties of bulk liquid Li, Al, and the Li-Na alloy [15].

OF-AIMD simulations for the liquid-vapor surfaces in Li and Na are presented for thermodynamic conditions near their respective triple points. We have considered slabs consisting of 2000 ions in a supercell with two free surfaces normal to the  $z$  axis. The dimensions of the slab were initially  $L_0 \times L_0 \times 2L_0$ , where  $L_0$  is chosen so that the average ionic number density of the slab coincides with the experimental bulk ionic number density of the system at the same temperature, i.e.,  $\rho_0(\text{Li}) = 0.04451 \text{ \AA}^{-3}$  and  $\rho_0(\text{Na}) = 0.02422 \text{ \AA}^{-3}$ , leading to  $L_0(\text{Li}) = 28.22 \text{ \AA}$  and  $L_0(\text{Na}) = 34.51 \text{ \AA}$ . A further  $8 \text{ \AA}$  of vacuum were added above and below the slab. Although the periodic boundary conditions require that a particle moving out of the cell in the  $z$  direction reappears on the other side of the slab, we have not observed this event during the present simulations.

Given the ionic positions at time  $t$ , the electron density was expanded in plane waves and the energy functional was minimized with respect to the plane-wave coefficients yielding the ground state electronic density, energy, and the forces on the ions, and finally the ionic positions and velocities were updated. For both systems, equilibration lasted for 15 ps and the cutoff energy for the plane-wave expansion was 6.95 Ry. The ionic time step for liquid Li was 0.0065 ps, and the calculation of properties was made averaging over another 80 ps. For liquid Na, the ionic time step was 0.010 ps and the calculation of properties was over 160 ps.

During the simulations, each slab contracted and the average ionic density rose in response to the condition of zero external pressure so that the density in the central region of the slab increased by  $\approx 7\%$  and  $\approx 10\%$  for Li and Na, respectively. The longitudinal ionic density profiles were computed from a histogram of particle positions relative to the slab's center of mass giving the results shown in Fig. 1. In both cases there is stratification for about five layers into the bulk liquid, a structural feature that has been observed experimentally for the liquid-vapor interface of Hg, Ga, In, K, and  $\text{Na}_{33}\text{K}_{67}$  [11]. The oscillations for Li, which is the higher density system, have a wavelength of  $\approx 2.5 \text{ \AA}$ ; for Na the oscillations have smaller amplitude and larger wavelength,  $\approx 3.0 \text{ \AA}$ . The wavelengths scale with the radii of the Wigner-Seitz spheres suggesting that the oscillations are due to atomic stacking against the surface. (Of course, the wavelengths also scale with  $k_F^{-1}$  for these monovalent metals, so ostensibly the wavelengths could be due to an electronic effect such as Friedel oscillations, but preliminary results for polyvalent metals show that it is the atomic radius rather than the Fermi surface radius that determines the oscillations.) For both systems, the first oscillation at the

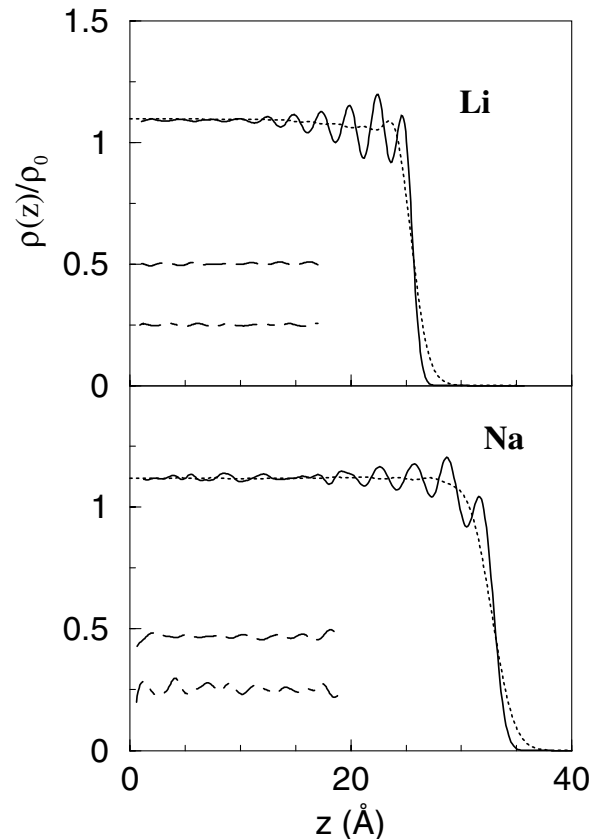


FIG. 1. Electronic (dotted line) and ionic (full line) density profiles normal to the Li and Na liquid-vapor interface. The densities are plotted relative to the bulk densities. The dashed and dot-dashed lines are the  $x$ -transverse (displaced by  $-0.5$ ) and  $y$ -transverse (displaced by  $-0.75$ ) ionic density profiles.

surface has a noticeably smaller amplitude than the second, in agreement with the MC results of Rice *et al.* [8] for Na and Cs, but at variance with the reported experimental ionic density profiles for Hg, Ga, and In where the first oscillation had the larger amplitude. Furthermore, as shown by Rice *et al.* [1,8], this stratification is not an artifact due to the finite size of the simulation box. We have computed the transverse ionic density profiles which, as seen in Fig. 1, are rather uniform with some noise which is substantially smaller than the amplitudes of the oscillations in the corresponding longitudinal ionic density profiles. On the other hand, using a central section of the slab of width 25 Å, we have calculated the corresponding pair distribution functions,  $g(r)$ , which are shown in Fig. 2 along with the experimental ones [17]. The small mismatch observed in Na stems from the increase in the ionic number density in the central part of the slab.

We have also examined how the stratification of the liquid-vapor interface affects the in-plane structure of the

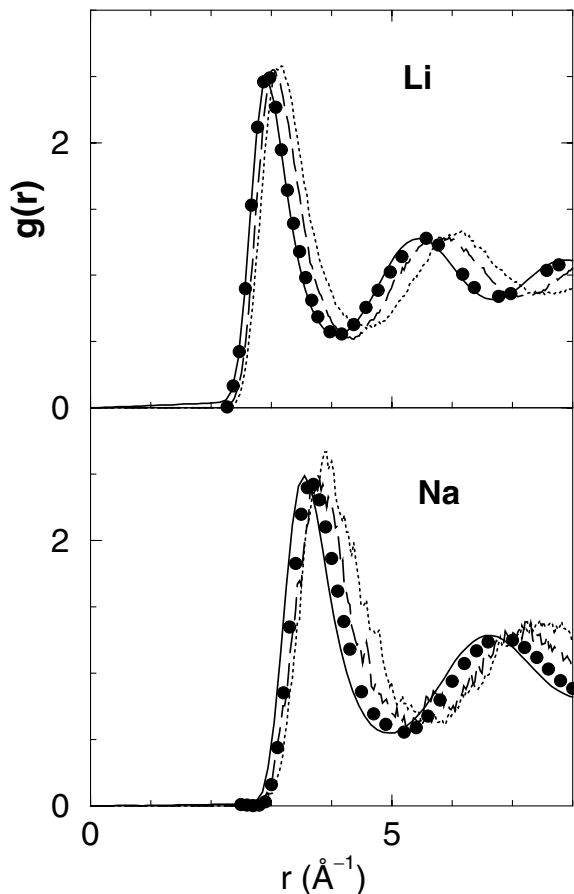


FIG. 2. Transverse pair correlation functions for selected layers of the Li and Na slabs, namely, from the bulk (full line), a slice from the outermost peak outwards (dotted line), and from the region between the outmost minimum and maximum (dashed line). The full circles are the experimental data [17].

liquid by evaluating the variation in the transverse pair correlation function across the interface. To this end, we divide the outer region of the slab into sections located between the minima and maxima of the oscillations. The results are also shown in Fig. 2. For Na the outer section is 1.6 Å wide and extends from the outermost maximum towards the inflection point in the ionic density profile; the next section extends from the outer maximum to the next minimum and is 1.2 Å wide. For Li both sections are 1.1 Å wide. On moving from section to section across the interface from the liquid to the vapor, there is a 10% total decrease in the Li ionic number density, whereas for Na it amounts to  $\approx 25\%$ . These decreases in ionic number density are reflected in the displacement towards greater  $r$  values of the corresponding  $g(r)$ . The larger displacement appears in Na which shows the greater decrease in density.

Further insight into the local structure is provided by the  $z$ -dependent coordination number  $n(z)$ , defined as the average number of neighbors within a distance  $r_m$  [identified as the position of the first minimum of the bulk  $g(r)$ ]. For both Li and Na, we obtain an average value  $n(z) = 11.8$  in most of their respective slabs, and only very close to the surfaces; namely, starting around the second outer maximum,  $n(z)$  begins to decrease. In fact, at the outer maximum  $n(z) = 7.8$  for Li [ $n(z) = 8.0$  for Na], whereas at the preceding maximum we have  $n(z) = 11.3$  for both metals. This decrease in  $n(z)$  is greater than that obtained in liquid Si by the KS-AIM calculations of Fabricius *et al.* [9]; in fact, the existence of some directional covalent bonding gave an  $n(z)$  changing from 6.4 in the bulk to 5.3 in the outer maximum.

The average electronic density profile shown in Fig. 1, also oscillates near the surface but with an opposite phase to the ionic oscillations and with a much smaller amplitude. Apart from some weak oscillations and, of course, the overall reduction, the liquid-vapor interface exerts a rather weak influence on the electronic density distribution. Also, we have taken the OF-AIMD generated ionic positions and constructed the linear superposition of the displaced electronic density used in the construction of the ionic pseudopotential. The corresponding electronic density profile, shown in Fig. 3, is very similar to the self-consistent OF-AIMD electronic profile, although this latter is slightly more spread out.

We have also performed a simulation of bulk liquid Na with 2000 ions in a cubic cell with periodic boundary conditions and at the same initial thermodynamic state as the slab. From the difference between the total energies in the bulk and the slab, we have estimated an average surface energy of  $\approx 228 \pm 15$  dyn/cm which is close to the experimental [18] surface tension ( $\approx 191$  dyn/cm), although a more detailed comparison would require the inclusion of the entropic effects.

The results of MD simulations of the liquid-vapor interface for liquid metals are presented. An *ab initio*

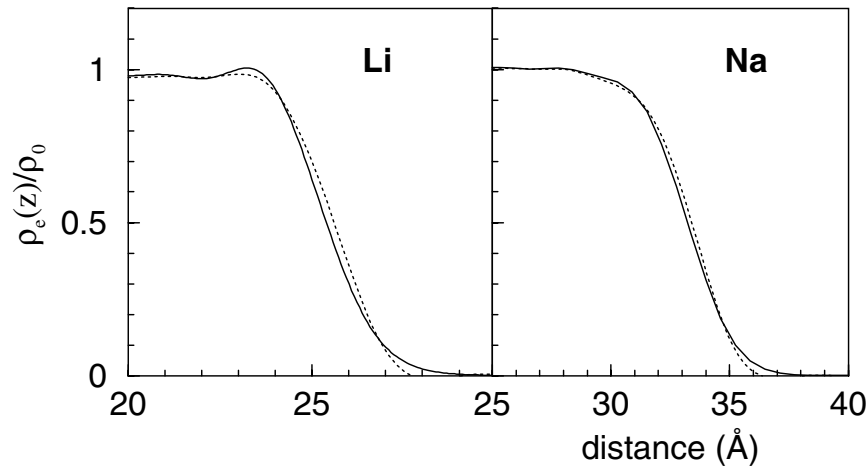


FIG. 3. Electronic density profiles (relative to the bulk average value) for the Li and Na liquid-vapor interfaces. The continuous line is the OF-AIMD result and the dashed line represents a linear superposition of displaced densities.

method was used which employs an approximate electronic kinetic functional, but which calculates the electronic structure and its influence of the forces on the ions at each step of the dynamics. Consequently, the large variations in electron density associated with the surface are accounted for in the forces. Results are presented for liquid Li and Na, based on slabs, composed of 2000 ions, which are wide enough to rule out interference effects between the two free surfaces, and in supercells which are large enough to eliminate slab-slab interactions. The electron and ion surface density profiles were calculated, and marked oscillations appear in the latter. For liquid Na, a value was also obtained for the surface energy which is in qualitative agreement with the measured surface tension coefficient. To our knowledge, only one other *ab initio* calculation of the liquid-vapor ionic density profile in a liquid metal has been performed. It used the KS-AIMD method which severely restricts the number of particles (96 ions), leading to a rather small slab ( $\approx 12$  Å thick) which may constrain its capability to simulate a real macroscopic liquid-vapor interface. However, these inconveniences are clearly overcome by the present OF-AIMD method, as shown in this communication.

D.J.G. acknowledges the financial support of the Ministerio de Educación, Cultura y Deporte of Spain, and the Physics Department at Queen's University. M.J.S. acknowledges the support of the NSERC of Canada.

[1] J.S. Rowlinson and B. Widom, in *Molecular Theory of Capillarity* (Clarendon, Oxford, 1982); D. Beaglehole, in *Fluid Interfacial Phenomena*, edited by C. A. Croxton (Wiley, New York, 1986); S. A. Rice, J. Gryko, and U. Mohanty, *ibid.*

[2] J. Penfold, *Rep. Prog. Phys.* **64**, 777 (2001).

[3] B. Groh, R. Evans, and S. Dietrich, *Phys. Rev. E* **57**, 6944 (1998); M. Gonzalez-Melchor, J. Alejandro, and F. Bresme, *Phys. Rev. Lett.* **90**, 135506 (2003).

[4] D. Beaglehole, *Phys. Rev. Lett.* **43**, 2016 (1979); *Physica (Amsterdam)* **B+C100**, 163 (1980).

[5] B.M. Ocko *et al.*, *Phys. Rev. Lett.* **57**, 94 (1986); Y. Martinez-Raton *et al.*, *Faraday Discuss.* **104**, 111 (1996).

[6] R. Evans, *Fundamentals of Inhomogeneous Fluids*, edited by D. Henderson (Dekker, New York, 1992).

[7] S.W. Barton *et al.*, *Nature (London)* **321**, 685 (1986).

[8] M.P. D'Evelyn and S.A. Rice, *Phys. Rev. Lett.* **47**, 1844 (1981); J.G. Harris, J. Gryco, and S.A. Rice, *J. Chem. Phys.* **87**, 3069 (1987); D.S. Chekmarev, M. Zhao, and S.A. Rice, *J. Chem. Phys.* **109**, 768 (1998); *Phys. Rev. E* **59**, 479 (1999).

[9] G. Fabricius *et al.*, *Phys. Rev. B* **60**, R16283 (1999).

[10] M.A. Gómez and E. Chacón, *Phys. Rev. B* **46**, 723 (1992); *Phys. Rev. B* **49**, 11405 (1994).

[11] O.M. Magnussen *et al.*, *Phys. Rev. Lett.* **74**, 4444 (1995); M.J. Regan *et al.*, *Phys. Rev. Lett.* **75**, 2498 (1995); E. DiMasi *et al.*, *Phys. Rev. B* **58**, R13419 (1998); *Phys. Rev. B* **59**, 783 (1999); H. Tostmann *et al.*, *Phys. Rev. B* **61**, 7284 (2000); O. Shpyrko *et al.*, *Phys. Rev. B* **67**, 115405 (2003).

[12] P. Hohenberg and W. Kohn, *Phys. Rev.* **136**, 864 (1964); W. Kohn and L.J. Sham, *Phys. Rev.* **140**, A1133 (1965).

[13] S. Iarlari *et al.*, *Surf. Sci.* **211/212**, 55 (1989).

[14] E. Chacon *et al.*, *Phys. Rev. Lett.* **87**, 166101 (2001); E. Velasco *et al.*, *J. Chem. Phys.* **117**, 10777 (2002).

[15] D.J. González *et al.*, *Phys. Rev. B* **65**, 184201 (2002); *J. Non-Cryst. Solids* **312–314**, 110 (2002).

[16] F. Perrot, *J. Phys. Condens. Matter* **6**, 431 (1994); E. Smargiassi and P.A. Madden, *Phys. Rev. B* **49**, 5220 (1994); M. Foley and P.A. Madden, *Phys. Rev. B* **53**, 10589 (1996).

[17] IAMP database of SCM-LIQ, Tohoku University. URL: <http://www.iamp.tohoku.ac.jp/database/>

[18] T. Iida and R. I. L. Guthrie, in *The Physical Properties of Liquid Metals* (Clarendon, Oxford, 1988).